Scroll Wave Instabilities in an Excitable Chemical Medium

Chaiya Luengviriya,[1,2] Ulrich Storb,[1] Gert Lindner,[3] Stefan C. Müller,[1] Markus Bär,[3] and Marcus J. B. Hauser[1]

[1]*Biophysics Group, Otto-von-Guericke-Universität Magdeburg, Universitätsplatz 2, 39106 Magdeburg, Germany*
[2]*Department of Physics, Kasetsart University, 50 Phaholyothin, Jatujak, Bangkok, 10900, Thailand*
[3]*Physikalisch-Technische Bundesanstalt, Fachbereich 8.4, Abbestraße 2-12, 10587 Berlin, Germany*

(Received 6 February 2007; published 9 April 2008)

Two kinds of scroll wave instabilities were studied experimentally in the excitable Belousov-Zhabotinsky reaction: three-dimensional meandering and negative line tension of the scroll wave filament. The filament displays a flat zigzag shape in the initial stages of the experiment. As the chemical medium ages, the filament assumes a wiggly shape while its length increases substantially. Numerical simulations underpin the experimental findings and their interpretation.

DOI: 10.1103/PhysRevLett.100.148302 PACS numbers: 82.40.Ck, 05.45.−a, 05.65.+b, 87.18.−h

Spiral waves were observed early on in quasi two-dimensional (2D) thin layers of a specific excitable chemical medium, the Belousov-Zhabotinsky (BZ) reaction [1,2]. The tip of such a spiral may either rotate rigidly on a circle with a single frequency or it may meander, involving two or more frequencies in its motion [2–4]. Scroll waves are the three-dimensional (3D) counterparts of spiral waves [5]. They can be characterized by the shape and topology of their filament, i.e., the line around which the scroll rotates. In 2D slices orthogonal to the filament, one finds rotating spirals. Their rotation phases may vary along the filament, leading to a twist. Scroll waves in external gradients were found experimentally to exhibit strong twists and complex dynamics [6]. Scroll wave dynamics were also implicated in biological phenomena like the 3D aggregation of slime molds [7] and ventricular fibrillation (VF) in the heart [8]. In particular, their potential impact in the development of VF has inspired many computational studies of 3D excitable media that have revealed numerous forms of complex dynamics ranging from twisted scrolls to spatiotemporal chaos [9–11]. The experimental study of scroll waves and their complicated dynamics remains a big challenge. The introduction of optical tomography [12] has allowed for detailed studies of twisted scroll waves [13] and scroll rings [14].

In parallel, simulations of simple models of excitable media have yielded different instabilities of simple straight scroll waves: namely, (i) a twist-induced instability known as ‘‘sproing’’[15], (ii) negative line tension of the filament [16], and (iii) a 3D form of meandering that leads not only to compound rotation in the plane, but also to a helical shape of the filament for periodic boundary conditions [17]. More recently, 3D meandering in systems with no-flux boundary conditions has been found to induce a planar zigzag shape of the filament [18]. The consequences of sproing include bending, as well as collision with and attachment of the filament to the boundary. These features have been experimentally observed in BZ systems subject to a gradient parallel to the filament [6,13]. The negative line tension instability can give rise to chaotic patterns denominated as ‘‘Winfree turbulence’’ [10(b)]. For straight scrolls in homogeneous media, linear stability analyses have been performed for all three types of instabilities [18] and for the experimentally relevant case of the sproing instability in a heterogeneous medium with a gradient parallel to the scroll filament [19]. Similar scroll wave instabilities have also been reported for the oscillatory complex Ginzburg-Landau equation, for instance, for the 3D analogue of a core instability reminiscent of meandering in excitable media [20] and for primary and secondary twist-induced instabilities [21].

In this Letter, we present a study of scroll wave instabilities in the BZ reaction in a closed container. 3D wave patterns were observed by optical tomography [12,13]. Closer analysis of the imaging data reveals filaments of flat zigzag shape, characteristic for 3D meandering in a system with closed boundaries, respectively, zero-flux boundary conditions [18]. In the long run, the medium ages and excitability decreases. This leads to a pronounced bending of the filament and a substantial increase of its length. Numerical simulations with a generic model [22,23] show that the zigzag shaped filament in the 3D meandering region starts to bend and lengthen as the excitability decreases and the region of negative line tension is approached. This supports the interpretation of the experimental results as a succession of two distinct instabilities due to 3D meandering and negative line tension.

Experimental.—A series of experiments was performed using a BZ reaction in a gel, prepared according to recipe IX of Ref. [24], which in 2D generates meandering spiral waves. Their low propagation velocity makes them suitable for detection by optical tomography [13,24]. The solution was placed into a cylinder of 21 mm diameter and a height of 25 mm. A scroll wave with straight filament was initiated by a partition method [6,13]. To prevent local inhibition by atmospheric oxygen and resulting spatial gradients [13], the reactor was sealed gas tightly shortly after creation of the scroll. This wave was observed in an

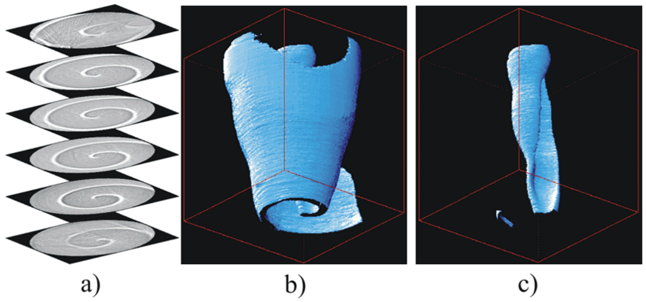

FIG. 1 (color online). Tomographic reconstruction of the scroll wave at 388 min: (a) A stack of six (out of 250) horizontal slices each of which contains a spiral wave. Isoconcentration surface of (b) the whole system and (c) the inner cylindrical volume with a diameter of 10 mm. The scroll wave has a zigzag filament and is weakly twisted which results in an upward cone shaped isoconcentration contour associated with three small ripples. The dimensions of the frames are $21 \times 21 \times 25\ \mathrm{mm}^3$.

optical tomographic setup which acquired 100 2D projections separated by 1.8° from each other. The resolution was $0.1\ \mathrm{mm\,pixel}^{-1}$ [13] and the temperature was kept constant at $22.0 \pm 0.1\ °\mathrm{C}$.

Examples of the tomographic reconstruction of the scroll wave are shown in Figs. 1 and 2. The 3D volume of the sample is divided into 250 horizontal slices, each of which contains a spiral wave [Fig. 1(a)]. The 3D structure of the scroll wave can be visualized as an isoconcentration surface. Such a reconstruction is presented in Figs. 1(b) for the whole volume while Fig. 1(c) shows the wave front near the filament.

To study the dynamics of the scroll wave, we estimated the wave filament for each rotation. We defined the filament as the line connecting the centers of spiral cores of the spirals in the 2D horizontal slices [Fig. 1(a)]. The cores, in turn, are the areas which are not invaded by the waves during one revolution of the spirals [2]. To characterize the dynamics of the filaments (Fig. 3), we have calculated the ratio of the filament length L to the height of the system L_z (Fig. 4).

The initial scroll wave exhibited a slightly tilted filament, roughly parallel to the vertical axis. Because of the initiation procedure, the uppermost part of the filament curved toward the horizontal. However, after ≈ 3 h the curved segment at the top vanished and the filament aligned itself approximately to the vertical axis. The relative filament length shrunk to $L/L_z \approx 1.2$ due to the positive line tension of the filament.

For $180 < t < 400$ min, the vertical filament assumed a zigzag shape, in line with predictions for 3D meandering behavior [18]. Its relative length L/L_z oscillated around $\approx$1.2 (Fig. 4). Furthermore, the phase of the uppermost spiral precedes that of the bottom spiral by an angle of $\approx \pi$ indicating a weakly twisted scroll wave [Fig. 1(a)]. The isoconcentration contour in Figs. 1(b) and 1(c) displays wiggles, which can be explained by the zigzag shape of the filament described above.

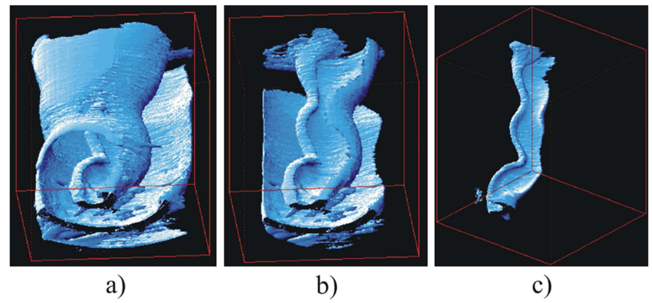

FIG. 2 (color online). Isoconcentration surface at 520 min: (a) of the whole system, and the inner cylindrical volumes with a diameter of (b) 16 mm and (c) 8 mm. The filament has extended leading to pronounced ripples at the wave front and to a zigzag shaped filament. Dimensions as in Fig. 1.

In the long time limit ($t > 400$ min), the filament has developed a more pronounced modulation (Fig. 3: 497 min) and its length increased substantially (Fig. 4). This indicates a negative line tension of the filament. Figure 2 shows the structure of the scroll wave close to the end of the experiment. The outermost [Fig. 2(a)] and inner wave fronts [Figs. 2(b) and 2(c)] now show much larger variations in the vertical directions reflecting the associated change of the filament in Fig. 3.

As the reaction ages during the experiment, the system passes two distinct interesting points. The first occurs at $t \approx 180$ min where the tilted filament becomes vertical, however, zigzag shaped, hence describing the 3D meandering instability. The second interesting point is reached at $t \approx 400$ min. Here the line tension becomes negative, leading to a considerable expansion of the filament length. Thus the experiment shows the occurrence of two distinct instabilities.

Modeling.—To connect our experimental observations with theoretical analysis of scroll wave instabilities, we have modeled the qualitative dynamics of scroll waves with the Barkley model [22], which reads

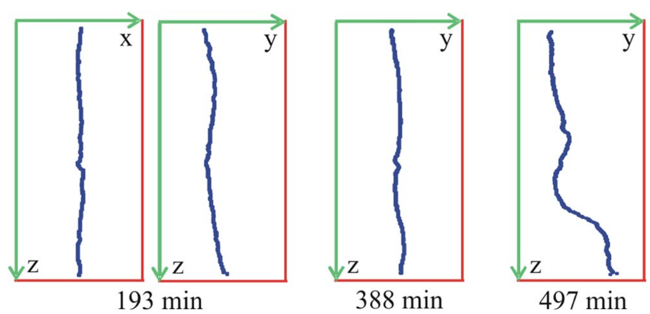

FIG. 3 (color online). Temporal development of the scroll wave filament. After a transient time of 3 h, the wave filament aligned almost vertically and became zigzag shaped (at 193 and 388 min). At $t = 193$ min the filament is almost straight in the xz plane while it shows a zigzag in the yz projection. In the long time limit, however, the filament expanded considerably in the yz plane (at 497 min). The dimensions of the frames are $12.5 \times 25\ \mathrm{mm}^2$.

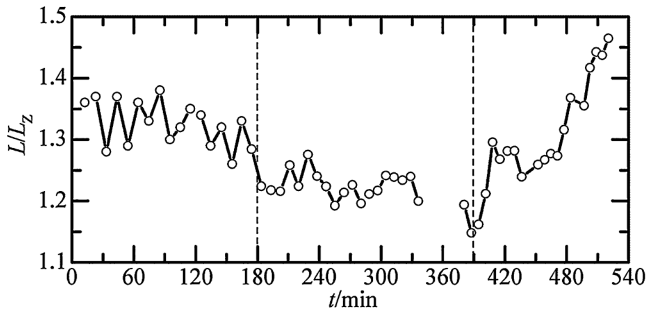

FIG. 4. Relative filament length L/L_z of the scroll wave. In the first ≈ 180 min, the filament length oscillates and contracts. For $180 < t < 400$ min, L/L_z oscillated around ≈ 1.2. Finally, in the long term limit, L/L_z increased substantially. At $340 < t < 370$ min, the observation was paused for a contrast enhancement purpose. The interval between two points corresponds to one rotation of the spiral around the filament.

$$\begin{aligned}\frac{\partial u}{\partial t} &= -\frac{1}{\epsilon}u(u-1)\left(u - \frac{v+b}{a}\right) + \nabla^2 u \\ \frac{\partial v}{\partial t} &= u - v + \delta\nabla^2 v.\end{aligned} \tag{1}$$

Zero-flux boundary conditions on the walls of the box were employed and a simple Euler-explicit forward integration scheme was used [23]. For the chosen parameters, a spiral period is roughly 4 time units while in the experiment rotation periods vary between 6 and 10 min. We choose the Barkley model with $\delta = 0$ because it is the only model where a linear stability analysis of straight scrolls has been performed [18] and simulation results can thus be related to known instabilities. The scenario reported below is generic and also appears in other models with decreasing excitability including the Oregonator model with $\delta = 0.6$ [25].

By linear stability analysis, three instabilities of scroll waves were found for different values of the excitability parameter a: 3D meandering, negative line tension, and spiroing [18]. The periodic modulation of the filament resulting from sproing in general exhibits a smaller wave number than the initial twist does [18]. In the course of the experiment, we observe a zigzag shape with 2.5 full rotations in the z direction; however, only a weak twist of $\approx \pi/L$, respectively, 0.5 full rotations along the z direction is found in the initial stage of the experiment (Fig. 1) ruling out a twist-induced instability as the origin of the zigzag shape. Hence, we start our simulations with a straight untwisted scroll with a small perturbation of the form $\cos(kz)$ added and mimic the aging of the solution in the experiment by a stepwise decrease in the excitability parameter a. We find a transition from straight scrolls with linear filaments to 3D meandering scrolls with zigzag shaped filaments as well as a notable stretching of the

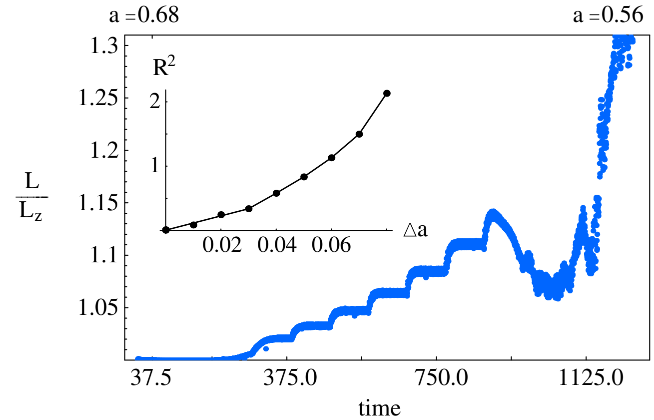

FIG. 6 (color online). Evolution of filament length in simulations of Eq. (1). Parameter a is decreased in equidistant steps of 0.01 from $a = 0.68$ at $t = 0$ to $a = 0.56$ at $t = 1218$. The inset shows the squared amplitude R^2 of the zigzag filament vs the distance Δa to the onset of 3D meandering obtained by a simulation run where a was increased from $a = 0.60$ to $a = 0.68$.

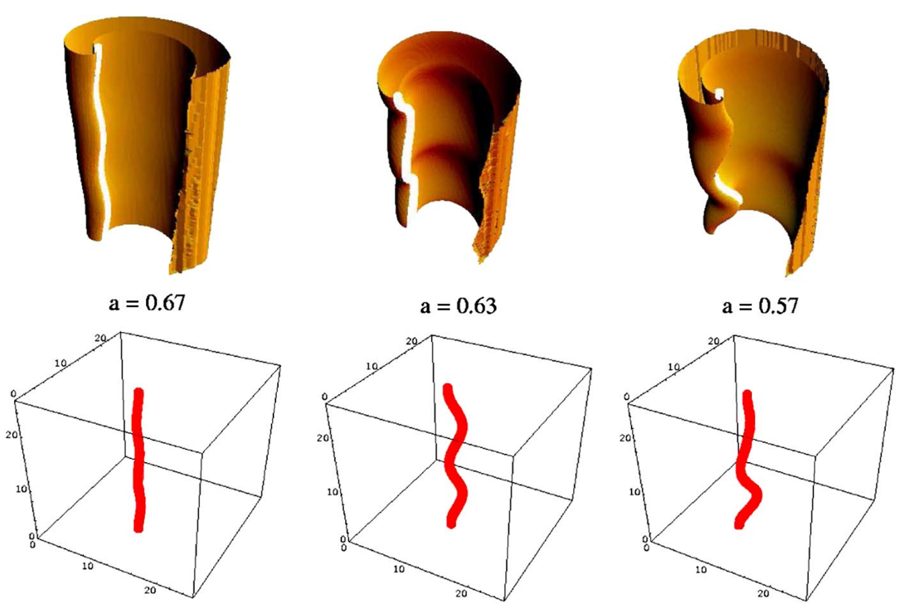

FIG. 5 (color online). Simulation results for different values of the excitability parameter a, shown are isoconcentration contours ($u = 0.5$) and filament shapes (obtained from the intersection of the contours $u = 0.5$ and $v = a/2 - b$). The left and middle panels show a scroll wave in the 3D meandering regime, the right panel indicates negative line tension and increase in filament length. Parameters: $b = 0.01$, $\epsilon = 0.025$. The volume of the simulation box is $25.6 \times 25.6 \times 26.0$. Numerical parameters: $\Delta x = 0.2$ and $\Delta t = 3.75 \times 10^{-3}$.

filament of the scroll wave upon decrease of a (Fig. 5). For the reverse simulation protocol (increasing a starting from zigzag shaped filaments at low values around $a = 0.60$), 3D meandering disappeared at $a_C = 0.68$, roughly in line with the value found in [18].

Similar to the experiment we have measured the filament length in the course of our simulation (Fig. 6). During the simulation run, the parameter a has been decreased stepwise from $a = 0.68$ to $a = 0.56$. We observe a related stepwise change of the filament length as a result of the 3D meandering instability. Stable zigzag shaped filaments with constant length are formed after short transients after each parameter change. The regular steps disappear below $a = 0.60$ leading to more twisted and initially shorter filaments as well as to irregular oscillations of the filament length. Finally, the filament length increases substantially for $a \leq 0.57$. This phenomenon appears in close vicinity to the negative line tension instability of straight scroll waves found previously at $a \approx 0.565$ [18]. Exploiting the backward run from $a = 0.60$ to $a = 0.68$ with increasing a, we also determined the amplitude R of the 3D meandering instability in dependence on $\Delta a = |a - a_C|$ and found the expected scaling $R^2 \propto \Delta a$ close to the instability (Fig. 6, inset).

The simulation results (Figs. 5 and 6) compare qualitatively well to the experimental findings (Figs. 1–4). After the transient, the experimental scroll wave shows initially clear signs of 3D meandering ($t \leq 388$ min), i.e., a flat moving zigzag shaped filament (Fig. 1) with $L/L_z > 1$, but roughly constant. By contrast, the increase of the filament length at long times (Fig. 2) is compatible with numerical simulations in the region of negative line tension (Figs. 5 and 6).

Discussion.—We have reported experiments on scroll wave dynamics in an excitable chemical medium using the BZ reaction in an optical tomography setup. Though the reaction was run in a closed container its aging proceeded only slowly, allowing for the observation of different regimes of scroll wave dynamics. Image processing was used to obtain both the isoconcentration surfaces during scroll wave rotation and the approximate shape and length of the scroll wave filaments. These data enabled us to distinguish different characteristic instabilities of straight scroll waves, namely, 3D meandering connected with a zigzag shaped filament and negative line tension indicated by a substantial increase in filament length and strong bending. In parallel, numerical simulations show that upon decrease of excitability (in the experiment due to ageing of the solution) a scroll wave indeed can pass from 3D meandering to a strongly nonlinear regime with irregular length fluctuations and finally substantially increasing filament length. To summarize, our work shows that optical tomography is capable of detecting instabilities of 3D patterns such as scroll waves. Numerical simulations connect the experiments to the theory of instabilities of scroll waves and suggest a direct relevance of the theory to the dynamics of 3D patterns in the BZ reaction.

We thank DFG (Grant No. MU884/17-1 as well as the SFB555 "Complex Nonlinear Processes") and the Graduiertenförderung des Landes Sachsen-Anhalt for financial support.

[1] A. T. Winfree, Science **175**, 634 (1972).
[2] S. C. Müller *et al.*, Science **230**, 661 (1985).
[3] D. Barkley, Phys. Rev. Lett. **68**, 2090 (1992); **72**, 164 (1994).
[4] Z. Nagy-Ungvárai *et al.*, Chaos **3**, 15 (1993); G. Li *et al.*, Phys. Rev. Lett. **77**, 2105 (1996).
[5] A. T. Winfree, Science **181**, 937 (1973); B. J. Welsh *et al.*, Nature (London) **304**, 611 (1983).
[6] A. M. Pertsov *et al.*, Nature (London) **345**, 419 (1990); S. Mironov *et al.*, J. Phys. Chem. **100**, 1975 (1996).
[7] O. Steinbock *et al.*, Proc. Natl. Acad. Sci. U.S.A. **90**, 7332 (1993).
[8] A. T. Winfree, Science **266**, 1003 (1994).
[9] F. Fenton and A. Karma, Phys. Rev. Lett. **81**, 481 (1998); Chaos **8**, 20 (1998).
[10] (a) Z. Qu *et al.*, Phys. Rev. Lett. **83**, 2668 (1999); (b) S. Alonso *et al.*, Science **299**, 1722 (2003); Phys. Rev. E **70**, 056201 (2004); (c) R. M. Zaritski and A. M. Pertsov, Phys. Rev. Lett. **92**, 168302 (2004); (d) A. Rusakov *et al.*, Phys. Rev. E **72**, 022902 (2005).
[11] R. H. Clayton *et al.*, Prog. Biophys. Molec. Biol. **90**, 378 (2006).
[12] A. T. Winfree *et al.*, Chaos **6**, 617 (1996); D. Stock and S. C. Müller, Physica (Amsterdam) **96D**, 396 (1996).
[13] U. Storb *et al.*, Phys. Chem. Chem. Phys. **5**, 2344 (2003).
[14] T. Bánsági and O. Steinbock, Phys. Rev. Lett. **97**, 198301 (2006).
[15] C. Henze *et al.*, Can. J. Phys. **68**, 683 (1990).
[16] V. N. Biktashev *et al.*, Phil. Trans. R. Soc. A **347**, 611 (1994).
[17] I. Aranson and I. Mitkov, Phys. Rev. E **58**, 4556 (1998).
[18] H. Henry and V. Hakim, Phys. Rev. Lett. **85**, 5328 (2000); Phys. Rev. E **65**, 046235 (2002).
[19] B. Echebarria *et al.*, Phys. Rev. Lett. **96**, 098301 (2006).
[20] I. S. Aranson *et al.*, Phys. Rev. E **57**, 5276 (1998).
[21] G. Rousseau *et al.*, Phys. Rev. Lett. **80**, 5671 (1998).
[22] D. Barkley, Physica (Amsterdam) **49D**, 61 (1991).
[23] M. Dowle *et al.*, Int. J. Bifurcation Chaos Appl. Sci. Eng. **7**, 2529 (1997).
[24] C. Luengviriya *et al.*, Phys. Chem. Chem. Phys. **8**, 1425 (2006).
[25] S. Alonso *et al.*, J. Phys. Chem. A **110**, 12 063 (2006).